Electronic Research Archive

https://www.aimspress.com/journal/era

ERA, 34(1): 583–605.
DOI: 10.3934/era.2026027
Received: 18 November 2025
Revised: 31 December 2025
Accepted: 08 January 2026
Published: 19 January 2026

Research article

A correction finite volume scheme preserving the discrete extremum principle for convection-diffusion equations on tetrahedral meshes

Fei Zhao[1,*], **Chan Bi**[1] **and Yao Yu**[2]

[1] College of Science, North China University of Technology, Beijing 100144, China

[2] College of Mathematics and System Science, Shandong University of Science and Technology, Qingdao 266590, China

* **Correspondence:** Email: zhaofei2020@ncut.edu.cn.

Abstract: In this paper, we present a nonlinear correction finite volume scheme that preserves the discrete extremum principle for convection-diffusion equations on tetrahedral meshes. The approximation of the diffusive flux is based on a nonlinear correction of the second-order linear flux, while the convection flux is approximated by the upwind scheme with second-order accuracy given by a Taylor expansion. In the construction of the new scheme, the requirement to represent auxiliary unknowns as convex combinations of primary unknowns can be removed, which greatly reduces the restrictions on diffusion coefficients and mesh geometry. Moreover, the obtained new scheme is cell-centered and satisfies local conservation. In addition, we theoretically testify that the numerical solution of the new scheme keeps the discrete extremum principle and verify it numerically. Numerical results also show that our scheme has almost second-order accuracy.

Keywords: convection-diffusion equation; extremum principle; tetrahedral meshes; second-order accuracy

1. Introduction

The convection-diffusion equation is a partial differential equation that describes the transfer of matter or energy in a fluid due to the combined effects of convection and diffusion mechanisms. It has a wide range of applications in physics, engineering, environmental science, and other fields, such as fluid dynamics, heat conduction, pollutant migration, semiconductor simulation, and so on. In many cases, computational meshes may have large aspect ratios or non-orthogonality, diffusion tensors may be strongly anisotropic, and models may have high Reynolds numbers, all of which can make numerical calculations difficult. There are some numerical simulations related to convection-diffusion problems, such as the domain decomposition method [1], the oscillation-free discontinuous Galerkin scheme [2],

and so on. The finite volume (FV) scheme has been widely studied by scholars due to its adaptability to complex geometry and strict conservation. So in this paper, we aim to construct an FV scheme for the convection-diffusion equation.

In the numerical solution of convection-diffusion equations, it is not only required that the scheme satisfies basic properties such as the stability, existence, uniqueness, and convergence of the solution, but also that the scheme preserves some physical properties of the equation, such as the local conservation, the positivity, and the discrete extremum principle. The property of preserving positivity can maintain the positivity of numerical solutions, and there has been a lot of literature on this topic over the past few decades; see [3–5] and the references therein. However, the schemes preserving positivity cannot maintain the upper bound of numerical solutions, which may lead to numerical oscillations. The scheme that preserves the discrete extremum principle not only maintains the physical bounds (including upper and lower bounds) of numerical solutions, but also avoids numerical oscillations [6]. Therefore, the schemes that satisfy this property are very robust.

The diffusion schemes that satisfy the discrete extremum principle on general meshes can be mainly divided into two categories. The first one is to construct a nonlinear scheme preserving extremum principle directly, and the scheme presented in [7] is a pioneer of this strategy. Based on this idea, two nonlinear FV schemes that satisfy the extremum principle on polygonal meshes are constructed in [6, 8]. Especially, the local maximum principle (LMP) structure has been firstly presented by the authors of [6], and they proved that any FV scheme possessing the LMP structure can satisfy the discrete maximum principle. Later, a number of nonlinear discrete extremum principle preserving schemes with the LMP structure were proposed (e.g., [9–11]). This type of extremum principle preserving diffusion scheme usually requires the introduction of auxiliary unknowns (such as cell vertex unknowns, face-centered unknowns, and the harmonic averaging points, etc.) in the construction of the scheme. Therefore, they often suffer from problems caused by auxiliary unknown interpolation. For example, in order to maintain the extremum principle without sacrificing the overall accuracy of the scheme, certain restrictions need to be added to the mesh geometry and diffusion coefficients. The second category is the correction approach. The authors of [12] constructed a nonlinear scheme that satisfies the discrete extremum principle by adding a certain nonlinear term to the linear scheme. The nonlinear scheme maintains some good numerical properties that are inherent in the original linear scheme, such as the local conservation and the coercivity. However, it has only first-order accuracy, even though the original scheme is second-order accurate. Afterwards, Le Potier [13] improved the symmetric and linear cell-centered FV scheme by using an updated second-order correction technique and obtained an extremum principle preserving scheme. The two-point fluxes scheme was corrected to obtain the extremum principle preserving scheme in [14]. The nonlinear correction method was also applied to the so-called nine-point scheme [15] to get discrete extremum principle preserving schemes for two-dimensional (2D) diffusion problems [16, 17] and a three-dimensional (3D) case [18].

The upwind approximation is one of the most popular methods for numerically approximating the convection flux, which is controlled by artificial viscosity [19] and different slope limiters [20–22]. The monotonic upstream-centered scheme for conservation laws (MUSCL) was introduced in [20]. Following this idea, the authors of [22] presented a new slope limiting technique that minimizes deviation of the reconstructed linear function from given values at selected points in each cell subject to some monotonicity constraints. Later, different slope limiting techniques were used to obtain

second-order upwind approximations (see [9, 10, 23]). A corrected upwind method was proposed in [4] to approximate the convection flux. The basic idea is that three points are chosen to reconstruct the gradient, and the Taylor series expansion at cell-edge to the cell-center is used to achieve the second-order accuracy.

In this paper, we construct a nonlinear correction FV scheme that preserves the discrete extremum principle for convection-diffusion equations on tetrahedral meshes. Following the method proposed in [4], an improved gradient reconstruction method for the 3D case is used to approximate the convection flux. Meanwhile, the diffusion scheme preserving a strong discrete extremum principle proposed in [18] is applied to discrete the diffusive flux. The obtained scheme is cell-centered and holds conservation. The new scheme can deal with anisotropic and discontinuous diffusion coefficient problems and is applicable to any tetrahedral mesh. It is worth remarking that in the derivation of the new scheme, the interpolation of auxiliary unknowns needs to have second-order accuracy without any other limitations, which is an improvement for many existing schemes [4, 10, 23]. Moreover, we confirm theoretically that the scheme satisfies the discrete extremum principle. In addition, we display some numerical tests to verify that the scheme not only satisfies the discrete extremum principle, but also obtains second-order accuracy.

The synopsis of this paper is arranged as follows: In Section 2, the problem and notation are provided. The nonlinear correction FV scheme preserving a discrete extremum principle is established in Section 3. The discrete extremum principle of numerical solution is proved in Section 4. Then in Section 5, some numerical tests are presented to verify the properties of the scheme. Finally, Section 6 closes this paper with conclusions.

2. Problem and notation

Consider the stationary convection-diffusion equation with unknown $u = u(x)$:

$$-\mathrm{div}(\kappa\nabla u - \vec{v}u) = f, \qquad \text{in } \Omega, \tag{2.1}$$

$$u = g, \qquad \text{on } \partial\Omega, \tag{2.2}$$

where Ω is a bounded polyhedral domain in $\mathbb{R}^3$ with boundary $\partial\Omega$. $\kappa = (\kappa_{ij}(x))$ is the viscosity scalar or tensor field, which satisfies the V-elliptic condition, i.e., there exist two positive constants λ and Λ such that $\lambda|\vec{\xi}|^2 \le \kappa_{ij}(x)\xi_i\xi_j \le \Lambda|\vec{\xi}|^2$ for a.e. $x \in \Omega$ and all $\vec{\xi} = (\xi_1, \xi_2, \xi_3)^T \in \mathbb{R}^3$. $\vec{v}(x)$ is the velocity field vector, $f(x)$ is a right-hand term, and $g(x)$ is a given boundary value function. To enable our numerical analysis, we make the following assumptions:

$$\mathrm{div}\vec{v}(x) \ge 0, \quad \vec{v}(x) \in C^1(\bar{\Omega})^3; \tag{2.3}$$

$$f(x) \in L^2(\Omega); \quad g(x) \in L^\infty(\Omega). \tag{2.4}$$

The solvability of the problem (2.1) and (2.2) can be traced back to [24], and their maximum and minimum principles are also sought out in [25].

In this paper, we divide the area Ω into tetrahedral meshes. The mesh cells and their cell-centers are denoted as $K, L, \cdots$. Here, the cell-center is taken as the centroid of the tetrahedron. Cell vertices are recorded as $A, B, C, \cdots$. The cell face is labeled as S, the cell face-center is marked as M, and the face-center is taken as the centroid of the triangle. In the event that the cell face S with vertices A, B, C is the common face of tetrahedron cells K and L, it is denoted as $S = K|L = ABC$; see Figure 1.

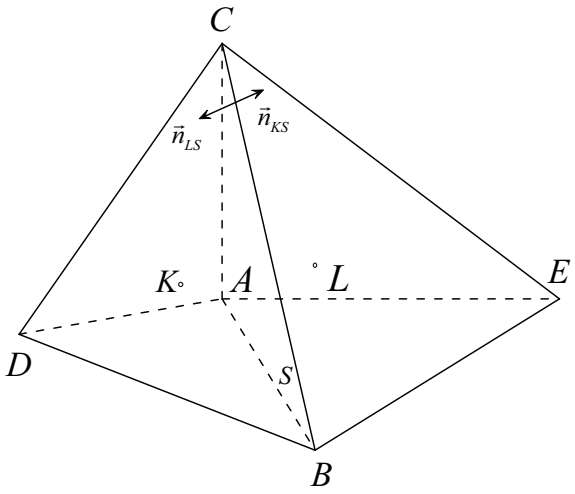

Figure 1. Notation related to two adjacent tetrahedron cells.

The set of all cells is marked as $\mathcal{J}$. Let $\mathcal{P}_{in}$ be the collection of cell-centers within Ω and $\mathcal{P}_{out}$ be the collection of cell face-centers on $\partial\Omega$. The set of all cell vertices is labeled as $\mathcal{N}$. The set of all cell faces is recorded as $\mathcal{E}$. Additionally, $\mathcal{E}_K$ represents the collection of all faces of cell K. Let $\mathcal{E}_{int} = \mathcal{E} \cap \Omega$ and $\mathcal{E}_{ext} = \mathcal{E} \cap \partial\Omega$. Denote $h = \left(\sup_{K\in\mathcal{J}} V(K)\right)^{\frac{1}{3}}$, where $V(K)$ is the volume of cell K. Suppose $\vec{n}_{KS}$ (resp. $\vec{n}_{LS}$) is the unit outer normal vector on the face S of cell K (resp. L), and it is tenable that $\vec{n}_{KS} = -\vec{n}_{LS}$ for $S = K|L$.

3. The construction of the correction scheme

Now, we construct the nonlinear correction FV scheme that maintains the discrete extremum principle.

Integrate (2.1) over cell K, and use the Gaussian formula to get

$$\sum_{S\in\mathcal{E}_K} (\mathcal{F}_{K,S} + \mathcal{G}_{K,S}) = \int_K f(x)\mathrm{d}x,$$

where

$$\mathcal{F}_{K,S} = -\int_S \nabla u \cdot \kappa^T \vec{n}_{KS}\,\mathrm{d}s, \tag{3.1}$$

and

$$\mathcal{G}_{K,S} = \int_S u\vec{v} \cdot \vec{n}_{KS}\,\mathrm{d}s. \tag{3.2}$$

3.1. Numerical discretization for the diffusion term

The diffusion scheme preserving a strong discrete extremum principle [4] is used to discrete the diffusion flux (3.1) in this subsection. For the sake of the completeness of this paper, here we only provide a brief description.

Assuming that starting from the cell-center K (resp. L), the ray along the direction of the vector $\kappa^T(K)\vec{n}_{KS}$ (resp. $\kappa^T(L)\vec{n}_{LS}$) intersects with the plane, where the triangle $S = \Delta ABC$ lies, at point K' (resp. L'), which is shown in Figure 2.

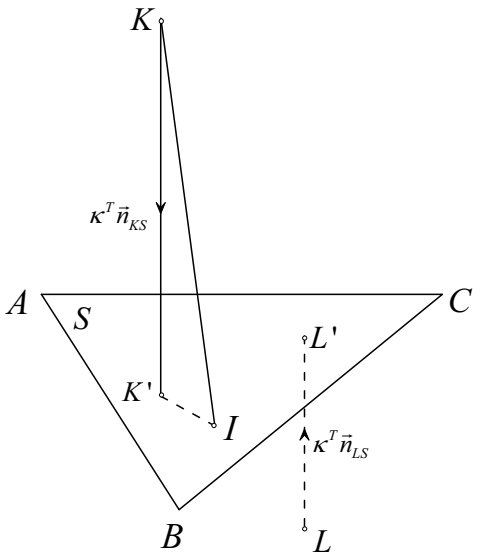

Figure 2. The discrete template of the linear flux.

By using the method in [26], the linear diffusion flux with second-order accuracy can be derived as

$$\hat{F}_{K,S} = \frac{|\kappa^T(K)\vec{n}_{KS}||\kappa^T(L)\vec{n}_{LS}||S|}{|\kappa^T(K)\vec{n}_{KS}||\overrightarrow{LL'}| + |\kappa^T(L)\vec{n}_{LS}||\overrightarrow{KK'}|}\Big[u_K - u_L - \frac{(u_A\vec{n}_{CB} + u_B\vec{n}_{AC} + u_C\vec{n}_{BA}) \cdot \overrightarrow{K'L'}}{2|S|}\Big], \tag{3.3}$$

where $\vec{n}_{CB}, \vec{n}_{AC}$, and $\vec{n}_{BA}$ respectively represent the cross product of the unit normal vector $\vec{n}$ to ΔABC and the vectors $\overrightarrow{CB}, \overrightarrow{AC}$, and $\overrightarrow{BA}$; see Figure 3.

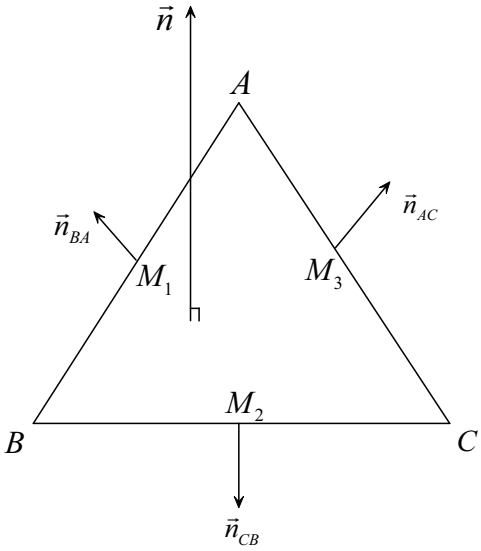

Figure 3. The face stencil.

Note that the scheme presented in [26] does not have the property of positivity or extremum principle due to the tangential part of the discrete normal flux (3.3). Therefore, the tangential part will be reconstructed to satisfy the discrete extremum principle.

Let $\mathcal{J}_K$ denote the set of cells around cell K, i.e., $\mathcal{J}_K = \{L \in \mathcal{J} | \overline{K} \cap \overline{L} \neq \emptyset\}$, where $\overline{K}$ represents the closure of cell K. Choose $K_{min} \in \mathcal{J}_K$ such that $u_{K_{min}} = \min\limits_{L\in\mathcal{J}_K} u_L$. It should be noted that the local minimum value may be achieved at several cells. At this time, if $u_K = \min\limits_{L\in\mathcal{J}_K} u_L$, we set $K_{min} = K$. Similarly, choose $K_{max} \in \mathcal{J}_K$ such that $u_{K_{max}} = \max\limits_{L\in\mathcal{J}_K} u_L$. Especially if $u_K = \max\limits_{L\in\mathcal{J}_K} u_L$, we also set $K_{max} = K$. Now, by modifying (3.3), we can obtain the single-sided flux with the LMP structure as follows:

$$\begin{aligned}\tilde{F}_{K,S} &= \tau_S(u_K - u_L + D_S) = \tau_S(u_K - u_L + D_S^+ - D_S^-)\\ &= \tau_S\Big[u_K - u_L + \frac{D_S^+}{u_K - u_{K_{min}} + \epsilon_0}(u_K - u_{K_{min}} + \epsilon_0) - \frac{D_S^-}{u_K - u_{K_{max}} - \epsilon_0}(u_K - u_{K_{max}} - \epsilon_0)\Big]\\ &\approx \tau_S(u_K - u_L) + g_{K,S}(U)(u_K - u_{K_m}),\end{aligned} \tag{3.4}$$

where

$$\begin{aligned}\tau_S &= \frac{|\kappa^T(K)\vec{n}_{KS}||\kappa^T(L)\vec{n}_{LS}||S|}{|\kappa^T(K)\vec{n}_{KS}||\overrightarrow{LL'}| + |\kappa^T(L)\vec{n}_{LS}||\overrightarrow{KK'}|} > 0,\\ D_S &= -\frac{(u_A\vec{n}_{CB} + u_B\vec{n}_{AC} + u_C\vec{n}_{BA})\cdot\overrightarrow{K'L'}}{2|S|},\\ D_S^+ &= \frac{|D_S| + D_S}{2} \geq 0, \qquad D_S^- = \frac{|D_S| - D_S}{2} \geq 0,\end{aligned}$$

$$g_{K,S}(U) = \begin{cases} \frac{\tau_S D_S^+}{u_K - u_{K_m} + \epsilon_0}, & D_S \geq 0,\\ \frac{\tau_S D_S^-}{u_{K_m} - u_K + \epsilon_0}, & D_S < 0,\end{cases} \qquad K_m = \begin{cases} K_{min}, & D_S \geq 0,\\ K_{max}, & D_S < 0,\end{cases}$$

$U = (u_K)_{K\in\mathcal{P}_{in}}$ is the vector composed of discrete unknowns, and ϵ_0 is a positive parameter that approximates the accuracy of the machine, used to avoid situations where the denominator is zero. In numerical experiments, we take $\epsilon_0 = 10^{-7}$.

Notice that $\hat{F}_{L,S} = \tau_S(u_L - u_K - D_S)$. Then we similarly redefine it as

$$\tilde{F}_{L,S} = \tau_S(u_L - u_K) + g_{L,S}(U)(u_L - u_{L_m}),$$

where

$$g_{L,S}(U) = \begin{cases} \frac{\tau_S D_S^+}{u_{L_m} - u_L + \epsilon_0}, & D_S \geq 0,\\ \frac{\tau_S D_S^-}{u_L - u_{L_m} + \epsilon_0}, & D_S < 0,\end{cases} \qquad L_m = \begin{cases} L_{max}, & D_S \geq 0,\\ L_{min}, & D_S < 0.\end{cases}$$

So for $S = K|L \in \mathcal{E}_{int}$, there are

$$\tilde{F}_{K,S} = \tau_S(u_K - u_L) + e_{K,S}(U), \tag{3.5}$$

$$\tilde{F}_{L,S} = \tau_S(u_L - u_K) + e_{L,S}(U), \tag{3.6}$$

where

$$e_{K,S}(U) = g_{K,S}(U)(u_K - u_{K_m}), \qquad e_{L,S}(U) = g_{L,S}(U)(u_L - u_{L_m}).$$

It can be seen that the single-sided fluxes (3.5) and (3.6) satisfy the LMP structure but have no local conservation. So then, we use a nonlinear harmonic average [7, 8] of $e_{K,S}(U)$ and $e_{L,S}(U)$ to obtain the conservative flux with the LMP structure. If $|e_{K,S}(U)| + |e_{L,S}(U)| \neq 0$, there are

$$\begin{aligned} F_{K,S} &= \tau_S(u_K - u_L) + \frac{|e_{L,S}(U)|}{|e_{K,S}(U)| + |e_{L,S}(U)|}e_{K,S}(U) - \frac{|e_{K,S}(U)|}{|e_{K,S}(U)| + |e_{L,S}(U)|}e_{L,S}(U), \\ F_{L,S} &= \tau_S(u_L - u_K) + \frac{|e_{K,S}(U)|}{|e_{K,S}(U)| + |e_{L,S}(U)|}e_{L,S}(U) - \frac{|e_{L,S}(U)|}{|e_{K,S}(U)| + |e_{L,S}(U)|}e_{K,S}(U). \end{aligned}$$

Moreover, if $|e_{K,S}(U)| + |e_{L,S}(U)| = 0$, we take $F_{K,S} = \tau_S(u_K - u_L)$ and define $F_{L,S}$ analogously. It is easy to see that $F_{K,S} + F_{L,S} = 0$.

Notice that regardless of whether $D_S \geq 0$ or $D_S < 0$, there hold $g_{K,S}(U) \geq 0$ and $g_{L,S}(U) \geq 0$. In the case of $D_S \geq 0$, there are $u_{K_m} = u_{K_{min}}$ and $u_{L_m} = u_{L_{max}}$. Therefore, we have $e_{K,S}(U)e_{L,S}(U) \leq 0$. In the case of $D_S < 0$, there are $u_{K_m} = u_{K_{max}}$ and $u_{L_m} = u_{L_{min}}$. We also have $e_{K,S}(U)e_{L,S}(U) \leq 0$. So, there is $|e_{L,S}(U)|e_{K,S}(U) = -|e_{K,S}(U)|e_{L,S}(U)$, and as a result, we have

$$F_{K,S} = \tau_S(u_K - u_L) + h_{K,S}(U)(u_K - u_{K_m}), \tag{3.7}$$

$$F_{L,S} = \tau_S(u_L - u_K) + h_{L,S}(U)(u_L - u_{L_m}), \tag{3.8}$$

where

$$h_{K,S}(U) = \begin{cases} \frac{2|e_{L,S}(U)|}{|e_{K,S}(U)|+|e_{L,S}(U)|}g_{K,S}(U), & \text{if } e_{K,S}(U)e_{L,S}(U) < 0, \\ 0, & \text{if } e_{K,S}(U)e_{L,S}(U) \geq 0, \end{cases}$$

$$h_{L,S}(U) = \begin{cases} \frac{2|e_{K,S}(U)|}{|e_{K,S}(U)|+|e_{L,S}(U)|}g_{L,S}(U), & \text{if } e_{K,S}(U)e_{L,S}(U) < 0, \\ 0, & \text{if } e_{K,S}(U)e_{L,S}(U) \geq 0, \end{cases}$$

and $h_{K,S}(U) \geq 0, h_{L,S}(U) \geq 0$.

For the case of $S \in \mathcal{E}_{ext}$, suppose the ray starting from the cell-center K, along the direction of vector $\kappa^T(K)\vec{n}_{KS}$, will not intersect with the discontinuity surface, and assuming that the ray intersects with the face $\bar{S} \in \mathcal{E}_{ext}$, the intersection point is marked as $K' \in \partial\Omega$. Whereupon, we have

$$F_{K,S} = -\frac{|\kappa^T(K)\vec{n}_{KS}||S|}{|\overrightarrow{KK'}|}(u_{K'} - u_K) = \delta_{K,S}(u_K - g(K')), \tag{3.9}$$

where $\delta_{K,S} = \frac{|\kappa^T(K)\vec{n}_{KS}||S|}{|\overrightarrow{KK'}|} > 0$.

3.2. Numerical discretization for the convection term

In this subsection, we apply a gradient reconstruction strategy based on the Taylor expansion, which is derived from the Patankar-type scheme proposed in [27], to complete the discretization of the convection part.

Recall that the face-center of $S = \Delta ABC$ is labeled as M, and the convection flux (3.2) can be rewritten as

$$\mathcal{G}_{K,S} = \int_S u\vec{v}\cdot\vec{n}_{KS}\,\mathrm{d}s \approx u_M \int_S \vec{v}\cdot\vec{n}_{KS}\,\mathrm{d}s = u_M v^+_{KS} - u_M v^-_{KS}, \tag{3.10}$$

where

$$v_{KS} = \int_S \vec{v}\cdot\vec{n}_{KS}\,\mathrm{d}s, \quad v^+_{KS} = \frac{|v_{KS}| + v_{KS}}{2} \geq 0, \quad v^-_{KS} = \frac{|v_{KS}| - v_{KS}}{2} \geq 0.$$

Distinctly, using u_M to approximate $u(M)$ in (3.10) does not maintain the upwind property. According to the standard upwind formula in [20], (3.10) should be written as

$$\mathcal{G}_{K,S} \approx v^+_{KS}\mathcal{W}_{K,S}(M) - v^-_{KS}\mathcal{W}_{L,S}(M), \tag{3.11}$$

where $\mathcal{W}_{K,S}(M)$ (resp. $\mathcal{W}_{L,S}$(M)) is the approximation with upwind property to cell K (resp. L) of the face-centered value $u(M)$.

In cell K (resp. L), starting from M, the ray along the direction of vector $\overrightarrow{MK}$ (resp. $\overrightarrow{ML}$) will definitely intersect with one of the faces of cell K (resp. L), which can be referred to as ΔADC (resp. ΔAEC), and the intersection point can be set as K_1 (resp. L_1) (see Figure 4).

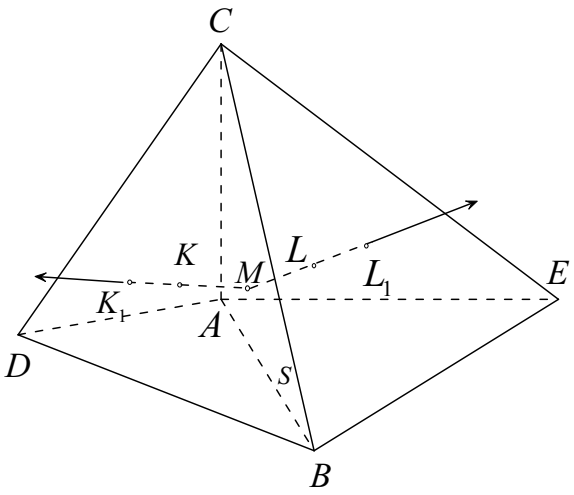

Figure 4. The approximate stencil for face-centered values.

By performing the Taylor expansion at the point K, there is

$$\mathcal{W}_{K,S}(M) = u_K + \nabla u|_K \cdot \overrightarrow{KM} + O(h^2). \tag{3.12}$$

Remark 1. *If u_K is a local minimum (resp. maximum) value, that is, $u_K \leq \min_{P\in\mathcal{N}_K} u_P$ (resp. $u_K \geq \max_{P\in\mathcal{N}_K} u_P$), where $\mathcal{N}_K$ is the collection of vertices composed of cell K, then $\nabla u|_K = 0$. The reason is a consequence of a well-known fact: If u is a continuous differentiable function in a domain Ω_0, and u achieves local minimum (or maximum) value at a point $K_0 \in \Omega_0$, then the gradient of u vanishes at the point K_0.*

Because $\overrightarrow{KM}$ and $\overrightarrow{K_1M}$ are collinear, the second item on the right end of (3.12) can be written as

$$\nabla u|_K \cdot \overrightarrow{KM} = \nabla u|_K \cdot \vec{t}_{KM}|\overrightarrow{KM}| = \nabla u|_K \cdot \vec{t}_{K_1M}|\overrightarrow{KM}| = \frac{|\overrightarrow{KM}|}{|\overrightarrow{K_1M}|}(u_M - u_{K_1}) + O(h^2), \tag{3.13}$$

where $\vec{t}_{KM}$ (resp. $\vec{t}_{K_1M}$) is the unit tangent vector along direction $\overrightarrow{KM}$ (resp. $\overrightarrow{K_1M}$).

Substituting (3.13) into (3.12) yields

$$\mathcal{W}_{K,S}(M) = u_K + \frac{|\overrightarrow{KM}|}{|\overrightarrow{K_1M}|}(u_M - u_{K_1}) + O(h^2),$$

where u_{K_1} can be approximated with second-order accuracy using the three vertex values on the triangular face where K_1 is located. Discard the higher term, and there is

$$W_{K,S}(M) = u_K + \frac{|\overrightarrow{KM}|}{|\overrightarrow{K_1M}|}(u_M - u_{K_1}).$$

It is obvious that $W_{K,S}(M)$ is the approximation with upwind property for u_M. Furthermore, to satisfy the discrete extremum principle, $\alpha_K \in [0, 1]$ is introduced into $W_{K,S}(M)$ as follows:

$$\widetilde{W}_{K,S}(M) = u_K + \alpha_K \frac{|\overrightarrow{KM}|}{|\overrightarrow{K_1M}|}(u_M - u_{K_1}) \tag{3.14}$$

such that

$$\min\{u_K, u_{P_i}\} \le \widetilde{W}_{K,S}(M) \le \max\{u_K, u_{P_i}\},$$

where $P_i \in \mathcal{N}_K$.

Remark 2. *Denote $u_{Pmin} = \min\{u_K, u_{P_i}\}$ and $u_{Pmax} = \max\{u_K, u_{P_i}\}$. Then α_K can be taken as*

$$\alpha_K = \begin{cases} \min\left\{1.0,\ \frac{|K_1M|}{|KM|}\frac{u_{Pmax}-u_K}{u_M-u_{K_1}}\right\}, & u_M - u_{K_1} > 0, \\ \min\left\{1.0,\ \frac{|K_1M|}{|KM|}\frac{u_{Pmin}-u_K}{u_M-u_{K_1}}\right\}, & u_M - u_{K_1} < 0, \\ 0, & u_M - u_{K_1} = 0. \end{cases}$$

Likewise, $\widetilde{W}_{L,S}(M)$ can also be written as

$$\widetilde{W}_{L,S}(M) = u_L + \alpha_L \frac{|\overrightarrow{LM}|}{|\overrightarrow{L_1M}|}(u_M - u_{L_1}). \tag{3.15}$$

Substitute (3.14) and (3.15) into (3.11). For the case of $S \in \mathcal{E}_{int}$, there is

$$G_{K,S} = \beta_{K,S}u_K - \beta_{L,S}u_L, \tag{3.16}$$

wherein

$$\beta_{K,S} = \nu^+_{KS}\frac{\widetilde{W}_{K,S}(M)}{u_K}, \qquad \beta_{L,S} = \nu^+_{LS}\frac{\widetilde{W}_{L,S}(M)}{u_L}.$$

If $u_K = 0$ (resp. $u_L = 0$), then $\beta_{K,S} = \nu^+_{KS}$ (resp. $\beta_{L,S} = \nu^+_{LS}$).

Remark 3. *Since* $\vec{n}_{KS} = -\vec{n}_{LS}$ *for* $S = K|L$*, so*

$$v_{LS} = \int_S \vec{v} \cdot \vec{n}_{LS} \mathrm{d}s = -v_{KS},$$

and then $v_{LS}^+ = v_{KS}^-, v_{LS}^- = v_{KS}^+$.

For the case of $S \in \mathcal{E}_{ext}$, it can also be derived as

$$G_{K,S} = \beta_{K,S} u_K - b_{K,S}, \tag{3.17}$$

in which $b_{K,S} = v_{KS}^- g(M) \geq 0$.

3.3. The treatment of the auxiliary unknown

During the construction of the scheme, in addition to basic unknowns, i.e., cell-centered unknowns, there are also auxiliary unknowns involved, including face-centered unknowns and vertex unknowns. By reason that the final scheme is a cell-centered one, these auxiliary unknowns demand to be interpolated by basic unknowns.

In now available literature (such as [4, 10, 21, 23]), in order to make the scheme have second-order accuracy and maintain the discrete extremum principle, the auxiliary unknowns demand to be represented as a convex combination of basic unknowns around at least second-order accuracy, which is extremely difficult to meet. If the interpolation method for auxiliary unknowns satisfies these two requirements, it usually has a relatively complex form, leading to a large amount of computation; or if it cannot satisfy both requirements simultaneously, restrictions will be imposed on the mesh properties and diffusion properties. Due to the correction of D_S in (3.4), our scheme no longer requires the auxiliary unknowns to be represented as convex combinations of basic unknowns, which is one of the innovations of this paper. Thus, we need only to express auxiliary unknowns as certain combinations of neighboring cell-centered unknowns with second-order accuracy.

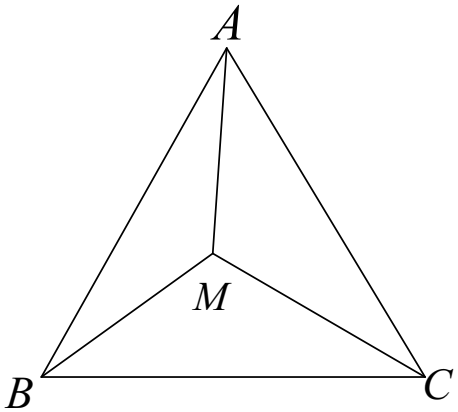

Figure 5. Interpolation template for face-centered unknowns.

Here, we employ the vertex calculation method in [28], which boasts second-order accuracy. However, it may potentially disrupt convex combinations. The numerical examples demonstrate that adopting this method does not compromise the ability of the scheme to preserve the discrete

extremum principle. Theoretically, other interpolation approaches with second-order accuracy are also viable. As for the face-centered unknown, it can be obtained through the area interpolation (see Figure 5). Specifically, as below:

$$u_M = \frac{m(\Delta MBC)}{m(\Delta ABC)}u_A + \frac{m(\Delta MAC)}{m(\Delta ABC)}u_B + \frac{m(\Delta MAB)}{m(\Delta ABC)}u_C,$$

where $m(\Delta ABC)$ expresses the area of ΔABC, and $m(\Delta MBC), m(\Delta MAC)$, and $m(\Delta MAB)$ are defined in the same way.

3.4. The FV scheme and its Picard iteration

With the expression of discrete diffusion and convection fluxes, the nonlinear correction FV scheme is derived as below:

$$\sum_{S\in\mathcal{E}_K}(F_{K,S} + G_{K,S}) = V(K)f_K, \qquad \forall K \in \mathcal{P}_{in}, \tag{3.18}$$

$$u_M = g(M), \qquad \forall M \in \mathcal{P}_{out}, \tag{3.19}$$

in which $f_K = f(K)$.

According to the scheme (3.18) and (3.19), we can obtain a system of algebraic equations: $M(U)U = N$, which is nonlinear. The nonlinear coefficient matrix $M(U)$ is composed of the coefficients of $F_{K,S}$ and $G_{K,S}$. Besides, N is the discrete vector, which is determined by the information of boundary conditions (3.19) and the right-hand term of (3.18).

Now, we iteratively solve the aforementioned nonlinear system by using the Picard iteration: Select the small positive parameter ε_{non} and the positive initial value vector U^0, and loop through the following process for $s = 1, 2, \cdots$

1) Solve the linear system $M(U^{(s-1)})U^{(s)} = N$.

2) Stop if $\|M(U^{(s)})U^{(s)} - N\| \le \varepsilon_{non}\|M(U^{(0)})U^{(0)} - N\|$.

The linearized system $M(U^{(s-1)})U^{(s)} = N$ can be solved by using the bi-conjugate gradient stabilized method [29]. When the relative norm of the initial residuals is less than ε_{lin}, the loop in this process terminates. In numerical examples, we take $\varepsilon_{non} = 10^{-6}$ and $\varepsilon_{lin} = 10^{-12}$.

4. The discrete extremum principle

Now, we declare our major conclusion that the new correction scheme maintains the discrete extremum principle. Let $u_{min} = \max\{0, \min_{K\in\mathcal{P}_{in}\cup\mathcal{P}_{out}} u_K\}$ and $u_{max} = \max\{0, \max_{K\in\mathcal{P}_{in}\cup\mathcal{P}_{out}} u_K\}$.

Theorem 4.1. *The nonlinear correction FV scheme (3.18) and (3.19) maintains the discrete extremum principle. That is to say,*

(i) in the case of $f \ge 0$, u_{min} can only be achieved on the boundary of domain Ω, only if $\{u_K|K \in \mathcal{P}_{in} \cup \mathcal{P}_{out}\}$ is constant;

(ii) in the case of $f \le 0$, u_{max} can only be achieved on the boundary of domain Ω, only if $\{u_K|K \in \mathcal{P}_{in} \cup \mathcal{P}_{out}\}$ is constant.

Proof. According to the diffusion fluxes (3.7) and (3.9), we obtain the diffusion terms of cell K:

$$\sum_{S\in\mathcal{E}_K} F_{K,S} = \sum_{S\in\mathcal{E}_K\cap\mathcal{E}_{int}} \Big(\tau_S(u_K - u_L) + h_{K,S}(U)(u_K - u_{Km})\Big) + \sum_{S\in\mathcal{E}_K\cap\mathcal{E}_{ext}} \Big(\delta_{K,S}(u_K - u_{K'})\Big), \tag{4.1}$$

where $\tau_S > 0, h_{K,S}(U) \geq 0$, and $\delta_{K,S} > 0$.

On the basis of the convection fluxes (3.16) and (3.17), we gain the convection terms of cell K:

$$\begin{aligned}\sum_{S\in\mathcal{E}_K} G_{K,S} &= \sum_{S\in\mathcal{E}_K\cap\mathcal{E}_{int}} \Big(\nu^+_{KS}\widetilde{W}_{K,S}(M) - \nu^+_{LS}\widetilde{W}_{L,S}(M)\Big) + \sum_{S\in\mathcal{E}_K\cap\mathcal{E}_{ext}} \Big(\nu^+_{KS}\widetilde{W}_{K,S}(M) - \nu^-_{KS}g(M)\Big)\\ &= \sum_{S\in\mathcal{E}_K} \nu^+_{KS}\widetilde{W}_{K,S}(M) - \sum_{S\in\mathcal{E}_K\cap\mathcal{E}_{int}} \nu^-_{KS}(\widetilde{W}_{L,S}(M) - u_K)\\ &\quad - \sum_{S\in\mathcal{E}_K\cap\mathcal{E}_{ext}} \nu^-_{KS}(g(M) - u_K) - \sum_{S\in\mathcal{E}_K} \nu^-_{KS}u_K,\end{aligned} \tag{4.2}$$

where $\nu_{KS} = \nu^+_{KS} - \nu^-_{KS}$, $\nu^+_{KS} \geq 0$, and $\nu^-_{KS} \geq 0$.

At present, let's consider the situation where $f \geq 0$. Suppose there is $K_0 \in \mathcal{P}_{in}$ such that $u_{K_0} = u_{min} \leq 0$. Then it will definitely be established by $u_{K_0} - u_L \leq 0$ for all $L \in \mathcal{P}_{in} \cup \mathcal{P}_{out}$. So in (4.1), due to $\tau_S > 0$, $h_{K_0,S}(U) \geq 0$, and $\delta_{K_0,S} \geq 0$, there are $\tau_S(u_{K_0} - u_L) \leq 0$, $h_{K_0,S}(U)(u_{K_0} - u_{K_0M}) \leq 0$, and $\delta_{K_0,S}(u_{K_0} - u_{K'}) \leq 0$, then $\sum_{S\in\mathcal{E}_{K_0}} F_{K_0,S} \leq 0$.

According to Remark 1, for all $S \in \mathcal{E}_{K_0}$, there have $\widetilde{W}_{K_0,S}(M) = u_{K_0}$. And by the initial assumption (2.3), there is

$$\sum_{S\in\mathcal{E}_K} \nu_{KS} = \sum_{S\in\mathcal{E}_K} \int_S \vec{v}\cdot\vec{n}_{KS}\,\mathrm{d}s = \int_K \mathrm{div}\vec{v}\,\mathrm{d}x \geq 0.$$

So, we have

$$\sum_{S\in\mathcal{E}_{K_0}} G_{K_0,S} = \sum_{S\in\mathcal{E}_{K_0}} \nu_{K_0S}u_{K_0} + \sum_{S\in\mathcal{E}_{K_0}\cap\mathcal{E}_{int}} \nu^-_{K_0S}(u_{K_0} - \widetilde{W}_{L,S}(M)) + \sum_{S\in\mathcal{E}_{K_0}\cap\mathcal{E}_{ext}} \nu^-_{K_0S}(u_{K_0} - g(M)) \leq 0.$$

Notice (3.18); it holds that

$$\sum_{S\in\mathcal{E}_{K_0}} F_{K_0,S} + \sum_{S\in\mathcal{E}_{K_0}} G_{K_0,S} = V(K_0)f_{K_0} \geq 0.$$

So, $\sum_{S\in\mathcal{E}_{K_0}} F_{K_0,S} = 0$. As $\tau_S > 0$, it has $u_L = u_{K_0}$, for $\forall L \in \mathcal{P}_{in} \cup \mathcal{P}_{out}$.

Therefore, unless u_K is a constant throughout the entire domain, this is a contradiction. Then, the case of $f \leq 0$ can be similarly proven. Hence, we finish the proof. □

5. Numerical examples

In this section, we provide several numerical examples to certificate the computational performance of our new scheme. The discrete extremum principle and convergent order are tested on two types of meshes (see Figure 6). Among which, Mesh A is obtained by first dividing the region Ω into n^3 cubes, and then dividing each cube into 24 uniform tetrahedrons, while Mesh B is obtained by dividing each

cube into 24 random tetrahedrons. The randomly distorted positions of vertices in Mesh B are defined as follows:

$$X = x_0 + \eta_x h, \quad Y = y_0 + \eta_y h, \quad Z = z_0 + \eta_z h,$$

where η_x, η_y, and η_z are random numbers between -0.3 and 0.3.

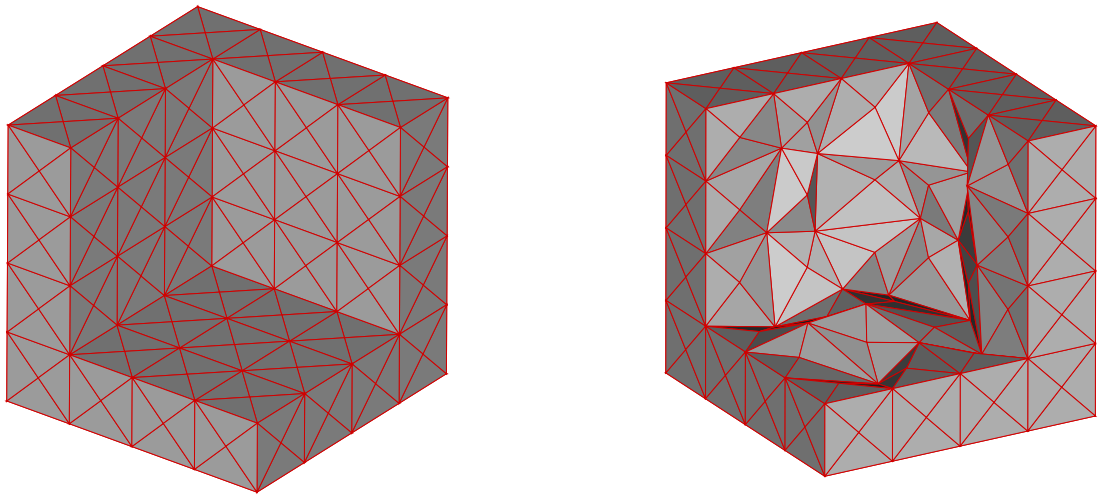

(a) Mesh A (b) Mesh B

Figure 6. Internal structure diagram of a tetrahedral mesh with size $h = 1/4$.

Here we apply the discrete L^2-norm to assess the approximate error between the numerical solution and the exact solution:

$$e_u = \Big[\sum_{K \in \mathcal{J}} (u(K) - u_K)^2 V(K) \Big]^{\frac{1}{2}},$$

where $u(K)$ represents the value of the exact solution at the cell-center K, while u_K represents the numerical solution at K.

The rate of convergence R_e is computed by the below formula (referred in [4]):

$$R_e = \frac{log[e_u(h_2)/e_u(h_1)]}{log(h_2/h_1)},$$

where h_1 and h_2 are the mesh sizes of two successive meshes and $e_u(h_1)$ and $e_u(h_2)$ are the corresponding discrete errors of the numerical solutions, respectively.

5.1. The discrete extremum principle

First, we verify the discrete extremum principle of our new scheme. Denote

$$u^{in}_{min} = \min_{K \in \mathcal{P}_{in}} u_K, \qquad u^{in}_{max} = \max_{K \in \mathcal{P}_{in}} u_K.$$

In other words, u^{in}_{min} (resp. u^{in}_{max}) denotes the minimum (resp. maximum) value of internal cells, and N_c denotes the number of cells.

5.1.1. The problem of diffusion dominance with $f = 0$

Now, we take into account the problem (2.1) and (2.2) on $\Omega = (0, 1)^3$. In this problem, the velocity field vector is set to $\vec{v} = (1, 1, 1)^T$, and the diffusion coefficient is chosen to

$$\kappa = \begin{pmatrix} \cos\theta & \sin\theta & 0 \\ -\sin\theta & \cos\theta & 0 \\ 0 & 0 & 1 \end{pmatrix} \begin{pmatrix} k_1 & 0 & 0 \\ 0 & k_2 & 0 \\ 0 & 0 & k_3 \end{pmatrix} \begin{pmatrix} \cos\theta & -\sin\theta & 0 \\ \sin\theta & \cos\theta & 0 \\ 0 & 0 & 1 \end{pmatrix},$$

where $k_1 = 1, k_2 = 0.1$, and $k_3 = 10$, $\theta = \frac{\pi}{6}$. The Dirichlet boundary condition is $g = x + \sin(\frac{\pi}{2}y) + z^2$, the right-hand term is $f = 0$, and the exact solution is unknown. On the basis of the discrete extremum principle, the maximum and minimum values of this problem are all reached on the boundary. Here, the minimum and maximum values on the boundary can be obtained as 0.0 and 3.0, respectively.

Table 1 gives the minimum and maximum values of our scheme on Mesh A and B, from which we can see that the minimum and maximum values are reached on the boundary. These results verify that our new scheme satisfies the discrete extremum principle on tetrahedral meshes.

Table 1. The maximum and minimum values of the diffusion dominance problem with $f = 0$.

N_c		24×4^3	24×8^3	24×12^3	24×16^3	24×24^3
Mesh A	u^{in}_{min}	1.564985×10^{-1}	6.753397×10^{-2}	4.247997×10^{-2}	3.088732×10^{-2}	1.993522×10^{-2}
	u^{in}_{max}	2.868769	2.936138	2.957734	2.968410	2.979013
Mesh B	u^{in}_{min}	1.567168×10^{-1}	6.755607×10^{-2}	4.250229×10^{-2}	3.088322×10^{-2}	1.993637×10^{-2}
	u^{in}_{max}	2.868572	2.936152	2.957694	2.968388	2.979007

5.1.2. The problem of convection dominance with $f = 0$

In this subsection, we consider the problem (2.1) and (2.2) on $\Omega = (0, 1)^3$ and take $\vec{v} = (1 - z, 1 - z, 1)^T$. The boundary condition is set as

$$g = \begin{cases} 1, & if\ 0 \le x, y \le 0.5, z = 0; \\ 0, & otherwise. \end{cases}$$

In this problem, $f = 0$, and the exact solution is unknown. However, it can be inferred from the discrete extremum principle that both its maximum value 1.0 and minimum value 0.0 are achieved on the boundary. The discrete extreme principle preserving scheme is used to solve this problem. The numerical solutions on Mesh A and B with the diffusion coefficient $\kappa = 0.1$ are shown in Figure 7. The maximum and minimum values of the new scheme are shown in Table 2, which reveals that the new scheme maintains the discrete extremum principle.

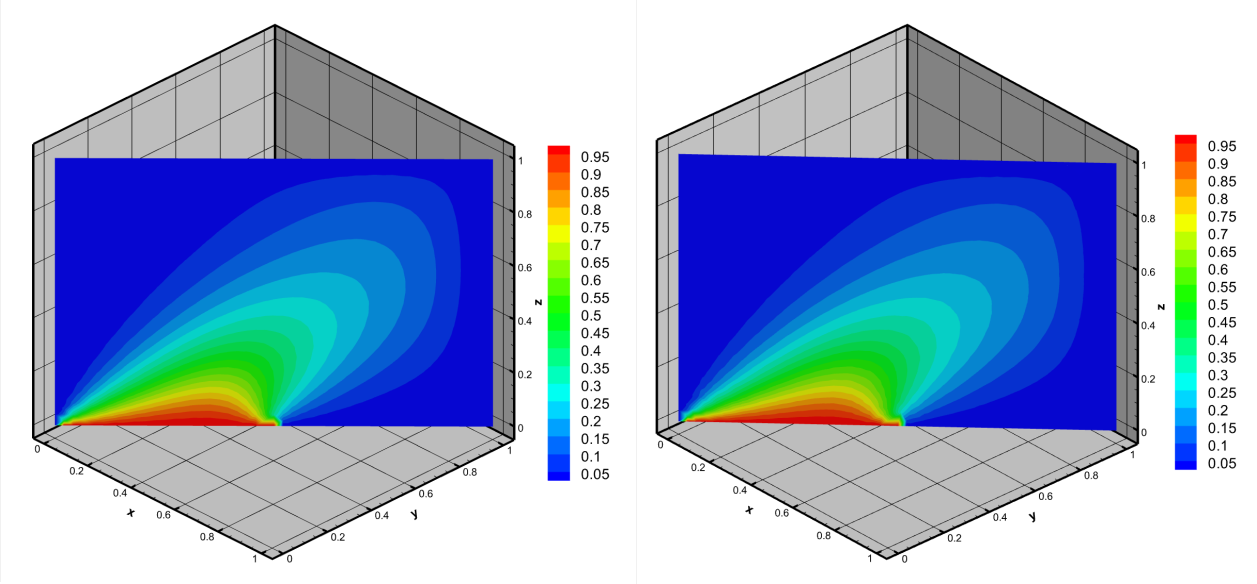

(a) on Mesh A (b) on Mesh B

Figure 7. The screenshots of the numerical solution on the plane where $x = y$.

Table 2. The maximum and minimum values of the convection dominance problem with $f = 0$.

N_c		24×4^3	24×8^3	24×12^3	24×16^3	24×24^3
Mesh A	u^{in}_{min}	6.745252×10^{-6}	3.317500×10^{-6}	9.364764×10^{-7}	3.896320×10^{-7}	1.150803×10^{-7}
	u^{in}_{max}	9.593711×10^{-1}	9.774463×10^{-1}	9.844215×10^{-1}	9.888563×10^{-1}	9.925758×10^{-1}
Mesh B	u^{in}_{min}	3.221821×10^{-6}	3.229276×10^{-6}	8.739608×10^{-7}	3.703387×10^{-7}	1.133482×10^{-7}
	u^{in}_{max}	9.569165×10^{-1}	9.772570×10^{-1}	9.843944×10^{-1}	9.888419×10^{-1}	9.925863×10^{-1}

5.1.3. The problem of convection dominance with $f > 0$ or $f < 0$

Here, we take into account the case of convection dominance in $\Omega = (0, 1)^3$. Set $\kappa = 10^{-5}$ and $\vec{v} = (1, 1, 1)^T$. The linear function $u = x + y + z$ serves as the exact solution, then the positive right-hand term and the Dirichlet boundary values can be calculated from the exact solution. The minimum value of this problem is 0.0, which can be reached on the boundary in light of the minimum principle.

Table 3 shows that the minimum value of this problem is indeed taken at the boundary. Moreover, it can be seen from the table that e_u can achieve machine accuracy, indicating that our scheme can maintain linearity.

Next, we consider the problem with a negative right-hand term. The computational domain, meshes, diffusion tensor, exact solution, and boundary conditions are the same as the previous problem. Set $\vec{v} = (-1, -1, -1)^T$, so there is negative right-hand term. Now, the maximum value of this problem is 3.0, which can also be reached on the boundary, according to the maxinum principle. The maximum values of this problem are shown in Table 4, which also show that the maximum value of this problem

is taken at the boundary and our scheme can maintain linearity.

Table 3. The minimum values of the problem with $f > 0$.

N_c		24×4^3	24×8^3	24×12^3	24×16^3	24×24^3
Mesh A	e_u	3.824493×10^{-8}	3.053807×10^{-8}	1.109510×10^{-8}	2.540190×10^{-8}	9.584987×10^{-9}
	u^{in}_{min}	2.187503×10^{-1}	1.093756×10^{-1}	7.291710×10^{-2}	5.468899×10^{-2}	3.645932×10^{-2}
Mesh B	e_u	1.935499×10^{-8}	5.733474×10^{-8}	8.295302×10^{-8}	1.603117×10^{-8}	9.600641×10^{-9}
	u^{in}_{min}	2.187501×10^{-1}	1.093750×10^{-1}	7.291667×10^{-2}	5.468750×10^{-2}	3.645833×10^{-2}

Table 4. The maximum values of the problem with $f < 0$.

N_c		24×4^3	24×8^3	24×12^3	24×16^3	24×24^3
Mesh A	e_u	4.195426×10^{-8}	7.338961×10^{-9}	1.620704×10^{-8}	8.563802×10^{-9}	3.740120×10^{-9}
	u^{in}_{max}	2.781250	2.890625	2.927083	2.945313	2.963542
Mesh B	e_u	5.028932×10^{-8}	2.562194×10^{-8}	2.265778×10^{-8}	1.873065×10^{-8}	4.439731×10^{-8}
	u^{in}_{max}	2.781250	2.890625	2.927083	2.945313	2.963542

5.2. The accuracy of the new scheme

In this section, we will provide several different types of examples defined on $\Omega = (0, 1)^3$ to verify the convergence order of the new scheme and compare it with the scheme proposed in [30] for the steady-state convection-diffusion equation. For the convenience of narration, we denote the discrete extremum principle preserving scheme here by DEP and the positivity preserving scheme in [30] by DPP.

5.2.1. Example 1

This example is a scalar diffusion coefficient problem, given as follows:

$$\vec{v} = (1, -1, -1)^T, \qquad \kappa = \begin{pmatrix} a & 0 & 0 \\ 0 & a & 0 \\ 0 & 0 & a \end{pmatrix}, \qquad u = x \cos\Big(\frac{\pi}{2}y\Big) \cos\Big(\frac{\pi}{2}z\Big),$$

where $a = 1.0, 10^{-2}, 10^{-4}$. f and g are given by (2.1) and (2.2).

Tables 5 and 6 display the L^2-norm of the error between the numerical solution and the exact solution for the new scheme with different diffusion coefficients on two meshes. From these tables, one can see that whether diffusion-dominated or convection-dominated, the solutions of both of the two schemes are able to achieve approximate second-order accuracy.

Table 5. Numerical results of Example 1 on Mesh A.

N_c			24×4^3	24×8^3	24×12^3	24×16^3	24×24^3
DEP	$a=1.0$	e_u	7.5021×10^{-4}	1.9402×10^{-4}	8.7542×10^{-5}	4.9650×10^{-5}	2.2260×10^{-5}
		R_e	–	1.95	1.96	1.97	1.98
	$a=10^{-2}$	e_u	1.8603×10^{-3}	3.7239×10^{-4}	1.4155×10^{-4}	7.1263×10^{-5}	2.7738×10^{-5}
		R_e	–	2.32	2.39	2.39	2.33
	$a=10^{-4}$	e_u	2.4648×10^{-3}	7.7156×10^{-4}	2.7233×10^{-4}	1.5120×10^{-4}	6.3419×10^{-5}
		R_e	–	1.68	2.57	2.05	2.14
DPP	$a=1.0$	e_u	7.5020×10^{-4}	1.9402×10^{-4}	8.7540×10^{-5}	4.9648×10^{-5}	2.2259×10^{-5}
		R_e	–	1.95	1.96	1.97	1.98
	$a=10^{-2}$	e_u	1.8604×10^{-3}	3.7135×10^{-4}	1.4150×10^{-4}	7.1241×10^{-5}	2.7700×10^{-5}
		R_e	–	2.32	2.40	2.38	2.33
	$a=10^{-4}$	e_u	2.4651×10^{-3}	5.8856×10^{-4}	2.5664×10^{-4}	1.4279×10^{-4}	6.2660×10^{-5}
		R_e	–	2.07	2.05	2.04	2.03

Table 6. Numerical results of Example 1 on Mesh B.

N_c			24×4^3	24×8^3	24×12^3	24×16^3	24×24^3
DEP	$a=1.0$	e_u	1.3178×10^{-3}	3.9438×10^{-4}	1.9931×10^{-4}	1.2184×10^{-4}	5.6830×10^{-5}
		R_e	–	1.74	1.68	1.71	1.88
	$a=10^{-2}$	e_u	2.4466×10^{-3}	5.1651×10^{-4}	2.0440×10^{-4}	1.0804×10^{-4}	4.2890×10^{-5}
		R_e	–	2.24	2.29	2.22	2.28
	$a=10^{-4}$	e_u	4.1330×10^{-3}	8.5881×10^{-4}	4.1196×10^{-4}	2.3445×10^{-4}	1.0386×10^{-4}
		R_e	–	2.27	1.81	1.96	2.01
DPP	$a=1.0$	e_u	1.3019×10^{-3}	4.3522×10^{-4}	2.1154×10^{-4}	1.2189×10^{-4}	5.6965×10^{-5}
		R_e	–	1.58	1.78	1.92	1.88
	$a=10^{-2}$	e_u	2.2792×10^{-3}	5.2538×10^{-4}	2.0722×10^{-4}	1.0680×10^{-4}	4.2837×10^{-5}
		R_e	–	2.12	2.29	2.30	2.25
	$a=10^{-4}$	e_u	3.0397×10^{-3}	8.5334×10^{-4}	3.8186×10^{-4}	2.1908×10^{-4}	9.9213×10^{-5}
		R_e	–	1.82	1.98	1.93	1.95

5.2.2. Example 2

Example 2 is a discontinuous diffusion coefficient problem, given as follows:

$$\vec{v}=(1,1,1)^T,\ \kappa=\begin{cases} ac, & x<\frac{1}{2},\\ a, & x\geq\frac{1}{2},\end{cases}\quad u=\begin{cases}\sin(\frac{\pi}{2}x)+\sin(\frac{\pi}{2}y)+\sin(\frac{\pi}{2}z), & x<\frac{1}{2},\\ 10\sqrt{2}\pi(x-\frac{1}{2})+\sin(\frac{\pi}{2}y)+\sin(\frac{\pi}{2}z)+\frac{\sqrt{2}}{2}, & x\geq\frac{1}{2},\end{cases}$$

where $c=40$ and $a=1.0, 10^{-2}, 10^{-4}$. f and g are given by (2.1) and (2.2).

Tables 7 and 8 represent the numerical results of Example 2 for different a on Mesh A and Mesh B, from which one can see that for the examples with a discontinuous coefficient, the solutions of the

new scheme are able to achieve approximate second-order accuracy. However, the DPP scheme does not converge in nonlinear iterations when $a = 1.0 \times 10^{-4}$ on both Mesh A and B.

Table 7. Numerical results of Example 2 on Mesh A.

N_c			24×4^3	24×8^3	24×12^3	24×16^3	24×24^3
DEP	$a = 1.0$	e_u	1.7540×10^{-3}	4.4190×10^{-4}	1.9696×10^{-4}	1.1095×10^{-4}	4.9379×10^{-5}
		R_e	–	1.99	1.99	1.99	2.00
	$a = 10^{-2}$	e_u	2.0507×10^{-3}	4.8362×10^{-4}	2.0534×10^{-4}	1.1094×10^{-4}	4.6333×10^{-5}
		R_e	–	2.08	2.11	2.14	2.15
	$a = 10^{-4}$	e_u	3.4141×10^{-3}	8.1871×10^{-4}	3.6025×10^{-4}	1.9987×10^{-4}	9.1005×10^{-5}
		R_e	–	2.06	2.02	2.05	1.94
DPP	$a = 1.0$	e_u	1.7539×10^{-3}	4.4190×10^{-4}	1.9693×10^{-4}	1.1094×10^{-4}	4.9378×10^{-5}
		R_e	–	1.99	1.99	1.99	2.00
	$a = 10^{-2}$	e_u	2.0502×10^{-3}	4.8365×10^{-4}	2.0537×10^{-4}	1.1096×10^{-4}	4.6390×10^{-5}
		R_e	–	2.08	2.11	2.14	2.15

Table 8. Numerical results of Example 2 on Mesh B.

N_c			24×4^3	24×8^3	24×12^3	24×16^3	24×24^3
DEP	$a = 1.0$	e_u	3.5704×10^{-3}	1.1715×10^{-3}	5.3357×10^{-4}	2.8751×10^{-4}	1.3912×10^{-4}
		R_e	–	1.61	1.94	2.15	1.79
	$a = 10^{-2}$	e_u	3.2743×10^{-3}	1.0196×10^{-3}	4.6501×10^{-4}	2.5945×10^{-4}	1.3782×10^{-4}
		R_e	–	1.68	1.94	2.03	1.56
	$a = 10^{-4}$	e_u	4.3164×10^{-3}	1.0848×10^{-3}	4.8584×10^{-4}	2.6981×10^{-4}	1.2076×10^{-4}
		R_e	–	1.99	1.98	2.04	1.98
DPP	$a = 1.0$	e_u	3.6921×10^{-3}	1.0750×10^{-3}	5.1267×10^{-4}	3.0486×10^{-4}	1.4109×10^{-4}
		R_e	–	1.78	1.83	1.81	1.90
	$a = 10^{-2}$	e_u	3.5544×10^{-3}	9.1508×10^{-4}	4.4746×10^{-4}	2.6102×10^{-4}	1.2182×10^{-4}
		R_e	–	1.96	1.76	1.87	1.88

5.2.3. Example 3

This example is a problem with an anisotropic diffusion coefficient described as

$$\vec{v} = (1, 1, 1)^T, \quad \kappa = \begin{pmatrix} 10a & 0 & 0 \\ 0 & 0.1a & 0 \\ 0 & 0 & a \end{pmatrix}, \quad u = \exp(xy) + z^2,$$

where $a = 1.0, 10^{-2}, 10^{-4}$. f and g are given by (2.1) and (2.2).

Tables 9 and 10 represent the numerical results of Example 3 for different a on Mesh A and Mesh B, from which one can see that whether diffusion-dominated or convection-dominated, the solutions of both of the two schemes are able to achieve approximate second-order accuracy.

Table 9. Numerical results of Example 3 on Mesh A.

N_c			24×4^3	24×8^3	24×12^3	24×16^3	24×24^3
DEP	$a=1.0$	e_u	3.3914×10^{-3}	1.0155×10^{-3}	4.7981×10^{-4}	2.7806×10^{-4}	1.2726×10^{-4}
		R_e	–	1.74	1.85	1.90	1.93
	$a=10^{-2}$	e_u	2.6985×10^{-3}	8.0531×10^{-4}	3.9422×10^{-4}	2.3515×10^{-4}	1.1180×10^{-4}
		R_e	–	1.74	1.76	1.80	1.83
	$a=10^{-4}$	e_u	4.4153×10^{-3}	1.1264×10^{-3}	5.0312×10^{-4}	2.8263×10^{-4}	1.2438×10^{-4}
		R_e	–	1.97	1.99	2.00	2.02
DPP	$a=1.0$	e_u	3.3914×10^{-3}	1.0156×10^{-3}	4.7996×10^{-4}	2.7819×10^{-4}	1.2697×10^{-4}
		R_e	–	1.74	1.85	1.90	1.93
	$a=10^{-2}$	e_u	2.6986×10^{-3}	8.0532×10^{-4}	3.9415×10^{-4}	2.3505×10^{-4}	1.1167×10^{-4}
		R_e	–	1.74	1.76	1.80	1.84
	$a=10^{-4}$	e_u	4.4157×10^{-3}	1.1268×10^{-3}	5.0346×10^{-4}	2.8295×10^{-4}	1.2468×10^{-4}
		R_e	–	1.97	1.99	2.00	2.02

Table 10. Numerical results of Example 3 on Mesh B.

N_c			24×4^3	24×8^3	24×12^3	24×16^3	24×24^3
DEP	$a=1.0$	e_u	5.3086×10^{-3}	1.9767×10^{-3}	9.9107×10^{-4}	5.8211×10^{-4}	2.6866×10^{-4}
		R_e	–	1.43	1.70	1.85	1.91
	$a=10^{-2}$	e_u	3.2210×10^{-3}	1.0776×10^{-3}	5.5404×10^{-4}	3.3539×10^{-4}	1.6740×10^{-4}
		R_e	–	1.58	1.64	1.74	1.71
	$a=10^{-4}$	e_u	5.2814×10^{-3}	1.4865×10^{-3}	6.9404×10^{-4}	4.0056×10^{-4}	1.8007×10^{-4}
		R_e	–	1.83	1.88	1.91	1.97
DEP	$a=1.0$	e_u	6.3679×10^{-3}	2.0150×10^{-3}	9.5792×10^{-4}	5.6580×10^{-4}	2.7271×10^{-4}
		R_e	–	1.66	1.83	1.83	1.80
	$a=10^{-2}$	e_u	3.1872×10^{-3}	1.0888×10^{-3}	5.4705×10^{-4}	3.3677×10^{-4}	1.6698×10^{-4}
		R_e	–	1.55	1.70	1.69	1.73
	$a=10^{-4}$	e_u	5.4691×10^{-3}	1.5205×10^{-3}	6.9866×10^{-4}	4.0241×10^{-4}	1.8173×10^{-4}
		R_e	–	1.85	1.92	1.92	1.96

5.2.4. Example 4

Example 4 presents problems with a nonconstant velocity field vector given as $\vec{v} = (\frac{1}{10}, \frac{z}{10}, -\frac{y}{10})$. The exact solution is $u = (1 - x^2)\sin y \exp(-z)$, and the diffusion tensor is $\kappa = 1$, which is diffusion-dominated, while the convection-dominated case is $u = x^2 \sin y \exp(-z)$ and $\kappa = 10^{-4}$.

The numerical results for the case of diffusion dominance are displayed in Table 11, while results for the case of convection dominance are displayed in Table 12. From these tables, one can see that for

both of the two cases, the solutions of our new scheme are able to achieve approximate second-order accuracy. However, the DPP scheme is not effective in dealing with steady-state nonconstant velocity field vector problems.

Table 11. Numerical results of Example 4 with diffusion dominance.

N_c			24×4^3	24×8^3	24×12^3	24×16^3	24×24^3
DEP	Mesh A	e_u	5.8820×10^{-4}	1.4370×10^{-4}	6.3375×10^{-5}	3.5509×10^{-5}	1.5720×10^{-5}
		R_e	–	2.03	2.02	2.01	2.01
	Mesh B	e_u	8.2196×10^{-4}	2.4569×10^{-4}	1.2277×10^{-4}	7.4302×10^{-5}	3.2177×10^{-5}
		R_e	–	1.74	1.71	1.75	2.06
DPP	Mesh A	e_u	1.0698×10^{-3}	7.7806×10^{-4}	7.4598×10^{-4}	7.3839×10^{-4}	7.3545×10^{-4}
		R_e	–	0.46	–	–	–
	Mesh B	e_u	1.3839×10^{-3}	8.5479×10^{-4}	7.6510×10^{-4}	7.5764×10^{-4}	7.4126×10^{-4}
		R_e	–	0.70	–	–	–

Table 12. Numerical results of Example 4 with convection dominance.

N_c			24×4^3	24×8^3	24×12^3	24×16^3	24×24^3
DEP	Mesh A	e_u	1.8444×10^{-3}	4.8843×10^{-4}	2.1399×10^{-4}	1.1686×10^{-4}	4.8693×10^{-5}
		R_e	–	1.92	2.04	2.10	2.16
	Mesh B	e_u	2.2058×10^{-3}	6.0426×10^{-4}	2.6608×10^{-4}	1.4989×10^{-4}	6.3812×10^{-5}
		R_e	–	1.87	2.02	1.99	2.11
DPP	Mesh A	e_u	5.3748×10^{-2}	5.3628×10^{-2}	5.3245×10^{-2}	5.2957×10^{-2}	5.2604×10^{-2}
		R_e	–	–	–	–	–
	Mesh B	e_u	5.3671×10^{-2}	5.3574×10^{-2}	5.3243×10^{-2}	5.2988×10^{-2}	5.2641×10^{-2}
		R_e	–	–	–	–	–

6. Conclusions

A nonlinear FV scheme preserving the discrete extremum principle for convection-diffusion equations with anisotropy and discontinuous diffusion coefficients on tetrahedral meshes is proposed, which can be regarded as an improvement of the existing schemes, such as the schemes in [4, 30]. In the process of the scheme construction, the diffusion term is discretized by employing the strong extremum principle preserving scheme in [18], while the convection term is discretized by applying the upwind scheme in [4, 30]. The obtained scheme keeps the discrete extremum principle and maintains conservation. More importantly, the construction of this scheme does not require that auxiliary unknowns are convex combinations of primary unknowns, which greatly reduces the

limitations on mesh properties and diffusion coefficients. Finally, numerical examples are used to verify the discrete extremum principle and second-order accuracy of the discrete solution.

We use the tetrahedral meshes in this paper, but the construction idea of this scheme can be generalized to general polyhedral meshes without essential difficulty. In particular, combined with the effective face technique described in [28], the approach of designing the scheme that satisfies the discrete extremum principle can be generalized to general polyhedral meshes with non-planar cell-faces.

Use of AI tools declaration

The authors declare they have not used Artificial Intelligence (AI) tools in the creation of this article.

Acknowledgments

This work is partially supported by the National Natural Science Foundation of China (12401505), R&D Program of Beijing Municipal Education Commission KM202210009005, Shandong Provincial Natural Science Foundation (ZR2021QA109).

Conflict of interest

The authors declare there are no conflicts of interest.

References

1. G. Xue, Y. Gao, Y. Yu, New domain decomposition algorithm for convection-dominated diffusion equations with the Samarskii scheme and the Jacobi explicit scheme, *J. Comput. Theor. Transp.*, **54** (2025), 205–226. https://doi.org/10.1080/23324309.2025.2461640
2. Y. Li, W. Zhao W. Zhao, An oscillation-free discontinuous Galerkin method for a nonlinear stochastic convection-dominated diffusion problem and its error analysis, *J. Comput. Math.*, **43** (2025), 1264–1289. https://doi.org/10.4208/jcm.2407-m2023-0265
3. K. Nikitin, Y. Vassilevski, A monotone nonlinear finite volume method for advection-diffusion equations on unstructured polyhedral meshes in 3D, *Russ. J. Numer. Anal. Math. Modell.*, **25** (2010), 335–358. https://doi.org/10.1515/rjnamm.2010.022
4. B. Lan, Z. Sheng, G. Yuan, A new finite volume scheme preserving positivity for radionuclide transport calculations in radioactive waste repository, *Int. J. Heat Mass Transfer*, **121** (2018), 736–746. https://doi.org/10.1016/j.ijheatmasstransfer.2018.01.023
5. G. Peng, A positivity-preserving finite volume scheme for convection diffusion equation on general meshes, *Int. J. Comput. Math.*, **99** (2022), 355–369. https://doi.org/10.1080/00207160.2021.1910943
6. J. Droniou, C. Le Potier, Construction and convergence study of schemes preserving the elliptic local maximum principle, *SIAM J. Numer. Anal.*, **49** (2011), 459–490. https://doi.org/10.1137/090770849

7. C. Le Potier, A nonlinear finite volume scheme satisfying maximum and minimum principles for diffusion operators, *Int. J. Finite Vol.*, **6** (2009), 1–20.
8. Z. Sheng, G. Yuan, The finite volume scheme preserving extremum principle for diffusion equations on polygonal meshes, *J. Comput. Phys.*, **230** (2011), 2588–2604. https://doi.org/10.1016/j.jcp.2010.12.037
9. K. Lipnikov, D. Svyatskiy, Y. Vassilevski, Anderson acceleration for nonlinear finite volume scheme for advection-diffusion problems, *SIAM J. Sci. Comput.*, **35** (2013), 1120–1136. https://doi.org/10.1137/120867846
10. Q. Zhang, Z. Sheng, G. Yuan, A finite volume scheme preserving extremum principle for convection-diffusion equations on polygonal meshes, *Int. J. Numer. Methods Fluids*, **84** (2017), 616–632. https://doi.org/10.1002/fld.4366
11. Z. Sheng, G. Yuan, Analysis of the nonlinear scheme preserving the maximum principle for the anisotropic diffusion equation on distorted meshes, *Sci. China Math.*, **65** (2022), 2379–2396. https://doi.org/10.1007/s11425-021-1931-3
12. C. Cances, M. Cathala,, C. Le potier, Monotone corrections for generic cell-centered finite volume approximations of anisotropic diffusion equations, *Numer. Math.*, **125** (2013), 387–417. https://doi.org/10.1007/s00211-013-0545-5
13. C. Le Potier, A second order in space combination of methods verifying a maximum principle for the discretization of diffusion operators, *C. R. Math.*, **358** (2020), 89–95. https://doi.org/10.5802/crmath.15
14. Y. Yu, G. Xue, A nonlinear correction finite volume scheme preserving maximum principle for diffusion equations with anisotropic and discontinuous coefficient, *Electron. Res. Arch.*, **33** (2025), 1589–1609. https://doi.org/10.3934/era.2025075
15. Z. Sheng, G. Yuan, A nine point scheme for the approximation of diffusion operators on distorted quadrilateral meshes, *SIAM J. Sci. Comput.*, **30** (2008), 1341–1361. https://doi.org/10.1137/060665853
16. W. Kong, Z. Hong, G. Yuan, Z. Sheng, Extremum-preserving correction of the nine-point scheme for diffusion equation on distorted meshes, *Adv. Appl. Math. Mech.*, **15** (2023), 402–427. https://doi.org/10.4208/aamm.OA-2021-0280
17. Z. Sheng, G. Yuan, A nonlinear scheme preserving maximum principle for heterogeneous anisotropic diffusion equation, *J. Comput. Appl. Math.*, **436** (2024), 115438. https://doi.org/10.1016/j.cam.2023.115438
18. F. Zhao, Z. Sheng, G. Yuan, A finite volume scheme preserving strong extremum principle for three-dimensional diffusion equations and its anderson acceleration, *J. Comput. Math.*, (2025), 1–27. https://doi.org/10.4208/jcm.2502-m2024-0081
19. G. Manzini, A. Russo, A finite volume method for advection-diffusion problems in convection-dominated regimes, *Comput. Methods Appl. Mech. Eng.*, **197** (2008), 1242–1261. https://doi.org/10.1016/j.cma.2007.11.014

20. B. van Leer, Towards the ultimate conservative difference scheme. V. A second-order sequel to Godunov's method, *J. Comput. Phys.*, **32** (1979), 101–136. https://doi.org/10.1016/0021-9991(79)90145-1

21. E. Bertolazzi, G Manzini, A second-order maximum principle preserving finite volume method for steady convection-diffusion problems, *SIAM J. Numer. Anal.*, **43** (2005), 2172–2199. https://doi.org/10.1137/040607071

22. K. Lipnikov, D. Svyatskiy, Y. Vassilevski, A monotone finite volume method for advection-diffusion equations on unstructured polygonal meshes, *J. Comput. Phys.*, **229** (2010), 4017–4032. https://doi.org/10.1016/j.jcp.2010.01.035

23. S. Wang, G. Yuan, Y. Li, Z. Sheng, A monotone finite volume scheme for advection-diffusion equations on distorted meshes, *Int. J. Numer. Methods Fluids*, **69** (2012), 1283–1298. https://doi.org/10.1002/fld.2640

24. S. Agmon, *Lectures on Elliptic Boundary Value Problems*, American Mathematical Society, 1965. https://doi.org/10.1090/chel/369

25. D. Gilbarg, N. S. Trudinger, *Elliptic Partial Differential Equtaions of Second Order*, Springer, 2001. https://doi.org/10.1007/978-3-642-61798-0

26. X. Lai, Z. Sheng, G. Yuan, A finite volume scheme for three-dimensional diffusion equations, *Commun. Comput. Phys.*, **18** (2015), 650–672. https://doi.org/10.4208/cicp.140813.230215a

27. H. Burchard, E. Deleersnijder, A. Meister, A high-order conservative Patankar-type discretisation for stiff systems of production-destruction equations, *Appl. Numer. Math.*, **47** (2003), 1–30. https://doi.org/10.1016/S0168-9274(03)00101-6

28. S. Wang, X. Hang, G. Yuan, A pyramid scheme for three-dimensional diffusion equations on polyhedral meshes, *J. Comput. Phys.*, **350** (2017), 590–606. https://doi.org/10.1016/j.jcp.2017.08.060

29. H. A. van der Vorst, Bi-CGSTAB: A fast and smoothly converging variant of Bi-CG for the solution of nonsymmetric linear systems, *SIAM J. Sci. Stat. Comput.*, **13** (1992), 631–644. https://doi.org/10.1137/0913035

30. F. Zhao, Z. Sheng, G. Yuan, A strong positivity-preserving finite volume scheme for convection-diffusion equations on tetrahedral meshes, *J. Appl. Math. Mech.*, **103** (2023), 202200032. https://doi.org/10.1002/zamm.202200032

AIMS Press